Spectroscopic Studies of a Phosphoinositide-Binding Peptide from Gelsolin: Behavior in Solutions of Mixed Solvent and Anionic Micelles

Wujing Xian,* Rolands Vegners,‡ Paul A. Janmey,§ and William H. Braunlin*
*Department of Chemistry, University of Nebraska-Lincoln, Lincoln, Nebraska 68588-0304, USA; ‡Latvian Organic Synthesis Institute, Riga, LV1006 Republic of Latvia; and §Experimental Medicine Division, Brigham and Women's Hospital, Harvard Medical School, Boston, Massachusetts 02115, USA

ABSTRACT The peptide G(150–169) corresponds to a phosphatidylinositol 4,5-bisphosphate (PIP_2) and filamentous actin (F-actin) binding site on gelsolin (residues 150–169, with the sequence KHVVPNEVVVQRLFQVKGRR). The conformation of this peptide in trifluoroethanol (TFE) aqueous solution was determined by ^1H nuclear magnetic resonance as the first step toward understanding the structural aspects of the interaction of G(150–169) and PIP_2. The circular dichroism experiments show that G(150–169) adopts a predominantly α-helical form in both 50% TFE aqueous solution and in the presence of PIP_2 micelles, therefore establishing a connection between the two conformations. ^1H nuclear magnetic resonance experiments of G(150–169) in TFE co-solvent show that the helical region extends from Pro-154 to Lys-166. The amphiphilic nature of this helical structure may be the key to understanding the binding of the peptide to lipids. Sodium dodecyl sulfate micelle solution is used as a model for anionic lipid environments. Preliminary studies of the conformation of G(150–169) in sodium dodecyl sulfate micelle solution show that the peptide forms an α-helix similar to but with some structural differences from that in TFE co-solvent. Fluorescence experiments provide evidence of peptide clustering over a narrow range of peptide/PIP_2 ratios, which is potentially relevant to the biological function of PIP_2.

INTRODUCTION

The ability of eukaryotic cells to move and to change shape in response to external stimuli is crucial for biological processes such as neuronal outgrowth, phagocytosis, platelet activation, and cytoplasmic transport. As a major component of the cellular cytoskeleton, actin filaments are essential for maintaining cell morphology and motility. The polymerization and depolymerization of filamentous actin (F-actin) is regulated by actin-binding proteins such as gelsolin. The polymerization of F-actin includes two steps, a slow nucleation process and a fast elongation process. Hence, the creation of new nuclei often becomes a limiting step for the rapid modification of the actin network. One of the roles of gelsolin and its homologs may be to provide a pool of such nuclei. Gelsolin binds to F-actin filaments and severs them, resulting in actin oligomers with gelsolin bound to their "barbed" or rapidly growing ends. Based on in vitro studies, it appears likely that when these gelsolin-actin complexes diffuse to the cytoplasmic membrane at sites where the phospholipids phosphatidylinositol phosphate (PIP) and phosphatidylinositol 4,5-bisphosphate (PIP_2) are generated, gelsolin dissociates from the actin oligomers. The oligomers may then serve as nuclei for rapid actin polymerization. The interaction between the phospholipids and gelsolin is crucial to this process. The binding of gelsolin to PIP and/or PIP_2 presumably involves electrostatic interactions between the positive charges on the protein and the negative charges on the phospholipid headgroups. However, the binding is not simply electrostatic, because it is not mimicked by other negative lipids such as phosphatidylserine and is affected in complex ways in mixed lipid vesicles also containing phosphatidyl-ethanolamine, or -choline (Janmey and Stossel, 1987). The preferential binding of gelsolin to PIP and PIP_2 is therefore hypothesized to require a special geometric arrangement between the binding site(s) on the protein and the lipid headgroups (Yu et al., 1992). At least two specific regions on gelsolin are regulated by PIP_2, and peptides based on the sequences of these sites are strong ligands for phosphoinositides. We have begun investigating the structural aspects of the interaction of one of these peptides with various lipids.

Gelsolin is a 85-kDa protein composed of six similar domains. Domains 1 and 4–6 show actin monomer binding activities, whereas domains 2 and 3 show filament side-binding activities (Janmey, 1993). Recently, the structure of the gelsolin segment 1 domain-actin complex has been solved by using x-ray crystallography (McLaughlin et al., 1993). The smallest fragment capable of severing actin filaments is segment 1 plus the 20 amino acids from the N-terminus of segment 2, which is one of the two PIP_2-regulated sites. This domain of 20 amino acids, G(150–169), competes efficiently with gelsolin for binding to PIP_2 and PIP (Janmey et al., 1992). The sequence of this peptide is KHVVPNEVVVQRLFQVKGRR. (Coordinates for the peptide have been deposited with the Protein Data Bank, ID number 1SOL.) Our initial studies described here have focused on the structure of this peptide in aqueous trifluoroethanol (TFE) solution. The peptide-PIP_2 interaction has been investigated by fluorescence studies to determine the role of the peptide structure in this interaction.

Circular dichroism (CD) is very useful for the rapid screening of secondary structures of peptides or proteins,

Received for publication 7 April 1995 and in final form 25 August 1995.
Address reprint requests to Dr. William H. Braunlin, Department of Chemistry, University of Nebraska, Hamilton Hall, Lincoln, NE 68588-0304. Tel.: 402-472-2228; Fax: 402-472-9402; E-mail: bill@toto.unl.edu.

0006-3495/95/12/2695/08 $2.00

and two-dimensional ^1H nuclear magnetic resonance (NMR) is ideal for obtaining conformational details that can be used for molecular modeling to help visualize possible conformations. In a system with peptides and phospholipids, however, interpretation of the NMR signal is complicated by motional line broadening. Precipitation of the peptide in PIP_2 micelle solutions also presents a problem for NMR studies because the precipitation occurs in the NMR concentration range. Therefore, for our initial studies we used TFE-water solutions to induce a stable structure in the peptide to mimic its PIP_2-bound conformation. We have also initiated studies of the interaction between the peptide and sodium dodecyl sulfate (SDS) micelles, and mixed micelles of PIP_2 and SDS. Because SDS micelles bear some resemblance to PIP_2 micelles, they should provide a reasonable control for electrostatic associations. Some preliminary data have been obtained for the peptide in the presence of SDS micelles and will be compared to the results obtained in aqueous TFE.

MATERIALS AND METHODS

Sample preparation

The peptide used for the CD experiments and some of the NMR experiments was synthesized using solid support chemistry by the Biotechnology Core Facility at the University of Nebraska-Lincoln. It was purified by high-pressure liquid chromatography on a preparative scale using a radical compression C-18 reverse-phase column (Waters, Milford, MA). The sample was eluted by a solvent gradient, with the more polar component being water with 0.1% trifluoroacetic acid (TFA), and the less polar component being 90% acetonitrile, 0.1% TFA and water. The eluent was collected manually. Acetonitrile and TFA were cleared by bubbling N_2 through the eluent. The solution was then lyophilized. The dried sample was subsequently dialyzed against 0.1 M NaCl with 10 mM Tris and 1 mM EDTA at pH 7.5 once, 10 mM NaCl at pH 7.5 twice, and finally water until EDTA was eliminated completely. The sample was lyophilized and stored at −20°C before use. The peptide used for other NMR experiments and for fluorescence measurements was obtained from the peptide synthesis facility of Harvard Medical School. Analytical high-pressure liquid chromatography of the peptide showed a single major peak with no other significant peaks. The peptide sample was dialyzed using the same procedures as described above and used without further purification. For the CD experiments, the lyophilized samples were dissolved in aqueous TFE solvent. The measured pH of the samples was always between 5.5 and 6.5. For the NMR experiments of G(150–169) in TFE co-solvent, 11.2 mg of the peptide was dissolved in 0.60 ml of 50% TFE/50% H_2O, to give a 7.4 mM solution whose pH was always between 5.5 and 6.0. For the preliminary experiments in SDS micelle solution, 7.4 mg of the peptide and 11.2 mg of per-deuterated SDS were dissolved in 0.5 ml of 20% D_2O/H_2O, to give a solution of 5.4 mM peptide and 80 mM SDS-d25, pH 6.5. PIP_2 was obtained from Sigma Chemical Company (St. Louis, MO) and used without further purification.

Circular dichroism experiments

CD experiments were performed on a Jasco 600 circular dichrometer at ambient temperature under N_2 atmosphere. The CD data were smoothed using J-600 software. The spectra were corrected by subtracting the spectra of the solvents from the spectra of the peptide solutions. Percentages of α-helix were estimated using a secondary structure prediction program included in the J-700 software, which was based on Yang's method (Yang et al., 1986). No significant change in CD profile was observed when the pH, buffer solution concentration, and peptide concentration were varied (data not shown).

NMR experiments

All NMR experiments were performed on the GE Omega 500 MHz NMR spectrometer in the Department of Chemistry at the University of Nebraska-Lincoln. A 5-mm reverse detection probe was used to obtain high proton sensitivity. The sample was locked on D_2O. The data were transferred to and processed on a SunSparc station 1+ using Omega software. The water resonance was suppressed by a pulse sequence that combined DANTE (Morris and Freeman, 1978) and SCUBA (Brown et al., 1988) pulse sequences. The presaturation time was set to 0.5–1.5 s, depending on the experiment performed. COSY spectra (Bax et al., 1981) were acquired using 1024 points for 512 increments, with 16 transient scans collected for each increment. The spectra were processed in the magnitude calculation mode. Time points in the acquisition dimension were multiplied by a sine-bell function with a period of 75%. Data for the evolution dimension were multiplied by a sine-square function with a period of 100%, and were zero filled to 1024 points. Phase-sensitive NOESY (Macura et al., 1982) spectra were obtained by acquiring 1024 points for 512 blocks, and 64 transient scans for each block. The free induction decay of the acquisition dimension was multiplied by a sine-bell function with a period of 75% and a phase shift of 60. The free induction decay of the evolution dimension was multiplied by the same function with a period of 100% and a 60° phase shift, and was zero filled to 1024 points. A series of mixing times ranging from 50 to 320 ms was used to observe the NOE build-up. Temperature variation was performed to differentiate some overlapping chemical shifts. Phase-sensitive total correlation spectroscopy (TOCSY) (Braunschweiler and Ernst, 1983; Bax and Davis, 1985) spectra were obtained by acquiring 1024 points for 512 blocks, with eight transient scans for each block. Spectra were processed in a manner identical to that employed for the NOESY spectra.

Molecular modeling

Molecular modeling experiments were performed on a Sun Sparc 1+ workstation using Sybyl from Tripos (St. Louis, MO). Volume integration was performed to determine a few selected crosspeak intensities for NOESY mixing times ranging from 50 to 320 ms. Distances between the γNHs of Asn-155, NH, and αH of Val-158 and the δHs of Pro-154 in a "perfectly" helical conformation were used as standard distances. Using the volume integration values of these crosspeaks as a reference, other crosspeaks were classified as strong, medium, or weak, corresponding to distance constraint ranges of 2.0–2.8 Å, 2.8–3.6 Å, and 3.6–4.8 Å, respectively. Initial structures were generated and minimized using a distance geometry algorithm (Crippen and Havel, 1988), with constraints due to bond distances, distances between atoms covalently bonded to the same atoms, and the NOE constraints. Fifty such structures were generated through random embedding. The best structures were selected and subjected to a restrained molecular dynamics (RMD) procedure. The standard Tripos force field (Clark et al., 1989) was used for the dynamics calculation. NOE constraints were applied using a force constant of 200 kcal/mol·A^2. Non-bonded interactions were truncated at 8 Å. Electrostatic interactions are not included in the force field. The RMD procedure was designed as an annealing process: each structure first underwent 500 fs of RMD at 300K, then was minimized using the method of steepest descent for 100 steps, followed by conjugated gradient minimization for 300 steps. The temperature was then raised to 1200K, where the structures underwent RMD for a total of 12,000 fs. The force constant for the NOE constraints was scaled down at the beginning to allow a time step of 1.5 fs, and was gradually increased to the default value. Afterward the temperature was decreased in steps of 50K until it reached 1000K; at each step 6000 fs of RMD was performed. The temperature was then decreased by 100K at a time until it reached 700K, and again at each step 6000 fs of RMD was performed. Finally, the temperature was decreased by 200K at a time until

it reached 300K, and again at each step 6000 fs of RMD was performed. The time step was 1.5 fs for the whole RMD procedure. The structures were then thoroughly minimized using first steepest descent and then conjugated gradient methods.

Fluorescence labeling and measurements

A portion of the G(150–169) peptide was elongated by the addition of an N-terminal cysteine to provide an anchor for fluorescence probes. This peptide was coupled to pyrene at the Peptide Synthesis laboratory of the Latvian Organic Synthesis Institute (Riga, Latvia). Four milligrams of Cys-G(150–169) and 30 mg of pyrene-maleimide bound to Celite (Molecular Probes, Eugene, OR) were suspended in 0.2 ml of aqueous solution containing 5 mM EGTA, and 0.2 ml of acetone was added. The pH was adjusted to 7.0 with sodium carbonate. The suspension was shaken for 6 h at room temperature and chromatographed on a 1 mm × 6 cm column of Sephadex LH-20. The peak of absorbance at 254 nm was collected, lyophilized, and resuspended in 10 mM Tris, pH 7.0, solution at a concentration of 160 μM. The concentration of pyrene-labeled peptide was determined by optical absorbance using an extinction coefficient of 36,000 at 343 nm (Haugland, 1992). Fluorescence spectra of solutions containing 2 μM pyrene-labeled peptide and various concentrations of different phospholipids were measured with a Perkin-Elmer LS50B instrument at 23°C. Fluorescence intensities are normalized to the emission peak at 384 nm of 2 μM peptide in the absence of lipids.

RESULTS

CD experiments

As judged by the CD profile, given in Fig. 1 *A*, which shows a characteristic negative peak at 200 nm, the peptide adopts a predominantly random coil conformation in water. As can also be judged from Fig. 1 *A*, in the presence of PIP_2, the conformation of the peptide changes to α-helix, as characterized by the positive absorption peak at 195 nm and the two negative absorption peaks at 207 nm and 222 nm, respectively. The CD spectrum of the peptide in SDS micelle solution (data not shown) is almost identical to that in PIP_2 micelle solution.

A similar trend of spectral changes was observed when the peptide was placed in a mixed solvent of water and TFE (Fig. 1 *B*). As the concentration of TFE in the solvent increased, the negative peak at 200 nm disappeared, and the peaks characteristic of the α-helical conformation appeared. In solution with 20% TFE, the peptide was already predominantly α-helical. The helicity increased further as the TFE concentration was increased to 40%. The peptide precipitated at TFE concentrations in excess of 60%.

NMR experiments

Resonances from individual residues were first identified according to amino acid type on the basis of TOCSY spectra. The connections between these residues were then traced in NOESY spectra starting from the fingerprint region containing three consecutive valines: 158, 159, and 160 (Wüthrich, 1986). In this manner, the chemical shifts of all of the residues were completely or partially assigned; these are listed in Table 1. The chemical shifts of a number

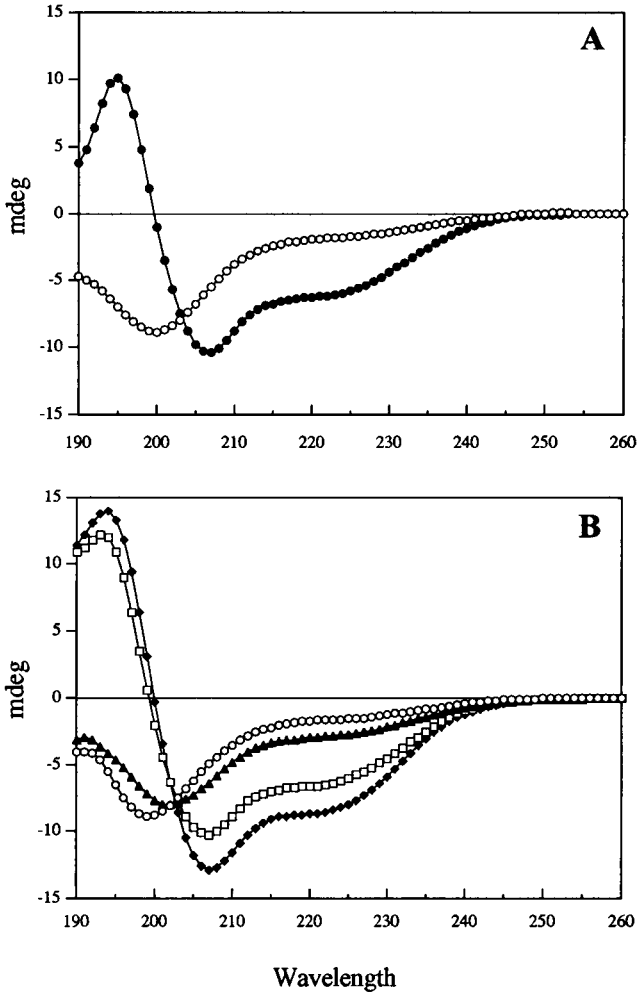

FIGURE 1 (*A*) CD spectra of 40 μM G(150–169) in phosphate-buffered water solution, pH 5.7 (○), and in 400 μM PIP_2 micelle solution, pH 6.0 (●). (*B*) CD spectra of 40 μM G(150–169) in water (○), 10% TFE (▲), 20% TFE (□), and 40% TFE (■). The pH of these solutions was always between 5.5 and 6.5.

of protons in α-helical conformation are noticeably different from those in the random coil conformation. The chemical shift differences for the α-protons ($CS_{\alpha\text{-helix}} - CS_{\text{random coil}}$) are displayed in Fig. 2.

As summarized in Fig. 3, for the central region of the peptide, NOESY experiments showed strong intra- and inter-residue crosspeaks. In this region, $d_{\alpha N}(i, i + 1)$ crosspeaks are very strong, and $d_{\alpha N}(i, i + 3)$ connections are well established. Some $d_{\alpha N}(i, i + 4)$ crosspeaks can be identified as well. Strong crosspeaks arise for the connection $d_{\alpha\beta}(i, i + 3)$. In the amide-amide region of the spectrum, $d_{NN}(i, i + 1)$ showed strong crosspeaks, and some $d_{NN}(i, i + 3)$ and $d_{NN}(i, i + 2)$ crosspeaks could be discerned as well.

Fluorescence measurements

In addition to intramolecular rearrangements of the peptides caused by PIP_2, this lipid can also promote peptide

TABLE 1 Proton chemical shifts (ppm) of gelsolin 150–169

Residue	NH	$C_\alpha H$	$C_\beta H$	$C_\gamma H$	$C_\delta H$	$C_\varepsilon H$	Others
Lys-1	8.46	4.95	3.21, 3.26	1.82	1.82	4.21	
His-2	8.29	4.86	3.13, 3.28				
Val-3	8.28	4.21	2.07	0.95			
Val-4	8.00	4.57	2.13	1.01			
Pro-5		4.41	2.04, 2.14	2.25, 2.43	3.71, 3.98		
Asn-6	8.32	4.49	2.82				$N_\gamma H$ 6.72, 7.49
Glu-7	9.08	4.00	2.12	2.40, 2.44			
Val-8	7.59	3.76	2.24	0.97, 1.07			
Val-9	7.45	3.60	2.22	0.97, 1.05			
Val-10	7.90	3.63	2.07	0.90, 1.04			
Gln-11	7.83	4.07	2.25	2.43, 2.62			$N_\delta H$ 6.60, 7.20
Arg-12	8.04	4.19	2.06	1.82	3.20, 3.27		$N_\varepsilon H$ 7.13
Leu-13	8.38	4.14	1.87	1.51	0.85		
Phe-14	8.34	4.40	3.26				
Gln-15	7.99	4.20	2.31	2.49, 2.66			$N_\delta H$ 6.66, 7.43
Val-16	8.04	4.01	2.26	1.01, 1.11			
Lys-17	8.25	4.30	1.91	1.54	1.70	2.98	
Gly-18	8.06	3.90, 4.01					
Arg-19	7.86	4.36	1.83, 1.95	1.70	3.22		$N_\varepsilon H$ 7.23
Arg-20	7.84	4.27	1.78, 1.92	1.67	3.24		$N_\varepsilon H$ 7.22

The chemical shifts are given in ppm and are referenced to TSP (0 ppm).

clustering at a critical ratio of peptide to lipid. Fig. 4 shows the fluorescence spectrum of pyrene-labeled G(150–169) in aqueous solution. This spectrum is typical of pyrene-labeled soluble compounds in having a major emission peak centered around 384 nm and a smaller peak around 404 nm. At a twofold excess of PIP_2 (2 μM peptide:4 μM PIP_2) these first two peaks are slightly enhanced and shifted to slightly higher wavelengths (387 and 407 nm), but most striking is the appearance of an intense broad emission maximum centered around 473 nm. Such a large high-wavelength emission is characteristic of pyrene excimer fluorescence (Haugland, 1992) due to stacking of the conjugated rings of the pyrene fluorophore at very small separations. When high concentrations of PIP_2 are added, the two low-wavelength peaks are strongly enhanced, but the high-wavelength peak diminishes. Fig. 5 shows that similar effects were seen with PI_4P and PI, but not with PS. The fluorescence enhancement of the first peaks (387 and 407 nm) appears to be caused by interaction of the peptides with any negatively charged lipid aggregate, but the clustering of the peptide appears to be specific for phosphoinositides.

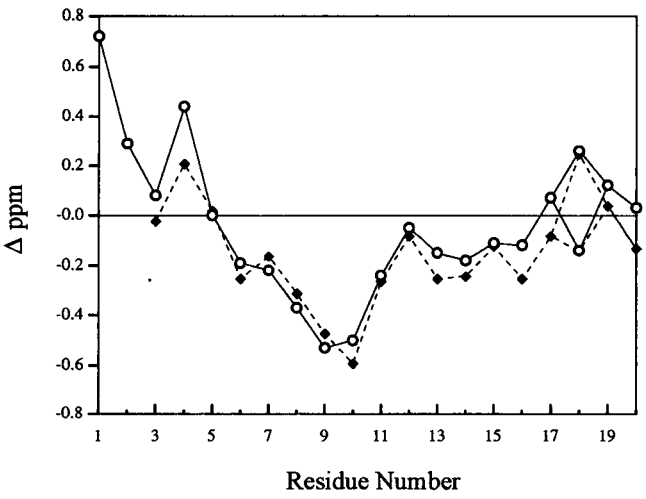

FIGURE 2 α-Proton chemical shift difference of G(150–169) between its conformation in 50% TFE solution and the random coil conformation ($CS_{50\%\ TFE} - CS_{random\ coil}$) (○), and that between the conformation in SDS micelle solution and the random coil conformation ($CS_{SDS} - CS_{random\ coil}$) (◆). Data of α-proton chemical shifts in random coil conformation are taken from Wishart (1991). Residues are numbered in sequential order. The missing points represent α-protons that were not observed.

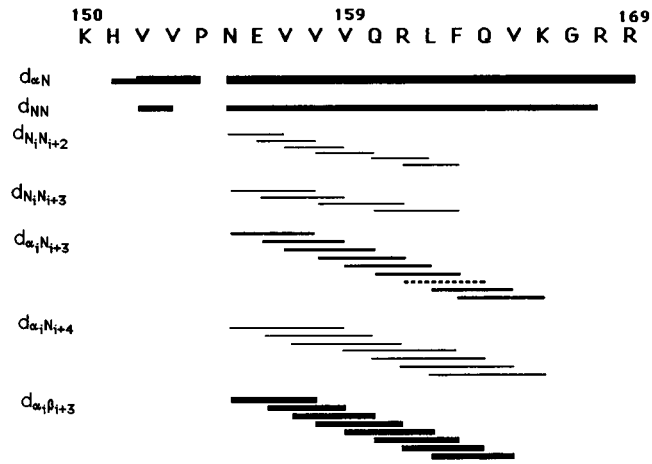

FIGURE 3 NOE connectivity patterns of G(150–169) as observed in NOESY experiments with 320 ms of mixing time. The intensities of the NOE crosspeaks are represented symbolically by the thickness of the lines connecting residue pairs.

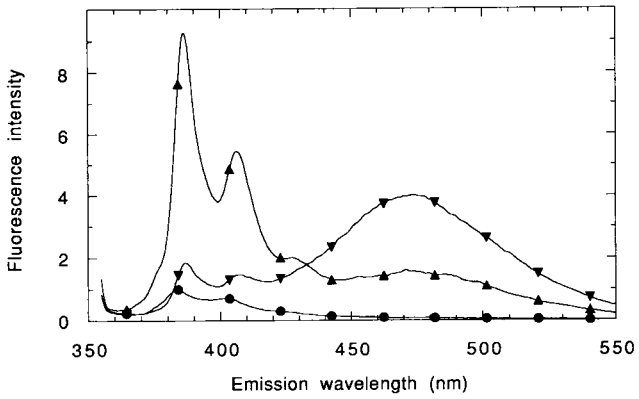

FIGURE 4 Fluorescence emission spectra with excitation at 343 nm of 2 μM pyrene-labeled Cys-G(150–169) in 10 mM Tris, pH 7.0, with various concentrations of PIP_2. The ratio of peptide:PIP_2 is 2 μM:0 μM (●), 2 mM:3.5 mM (▼), and 2 mM:56 mM (▲), respectively.

DISCUSSION

CD experiments

TFE is widely used to induce α-helix formation in oligopeptides (Sönnichsen et al., 1992). The mechanism by which TFE exerts this effect is only partially understood. One hypothesis is that the low dielectric constant of TFE mimics the hydrophobic environment of a protein. However, this hypothesis is at odds with the observation that charged group stabilization/destabilization of α-helices is not greatly affected by TFE concentration (Nelson and Kallenbach, 1986). Another proposed mechanism is that the weaker basicity of TFE weakens the hydrogen bonding of amide protons to the solvent, which in turn favors intramolecular hydrogen bonds and results in stabilized secondary structures (Llinas and Klein, 1975; Nelson and Kallenbach, 1986). Even though the driving force behind the helix-coil transition for the peptide in TFE mixed solvent might differ from that in PIP_2 solutions, the CD experiments reported here suggest that the helical conformations are similar in these two cases. Therefore it is reasonable to use the TFE-water mixed solvent system as a first step toward understanding the conformational transition of G(150–169) and its role in the peptide-PIP_2 interaction.

A further step is to study the peptide in SDS micelle solution. Such a solution provides a model environment closer to PIP_2 than does TFE co-solvent. The peptide shows nearly identical CD profiles in both PIP_2 and SDS micelle solution. This implies that the conformations of G(150–169) induced by SDS and PIP_2 are almost certainly similar. This similarity most likely reflects a similarity of electrostatic interactions between negatively charged lipid head groups and positive charges on the peptide side chains. Moreover, interactions between the hydrophobic core of the micelles and the hydrophobic side chains of the peptide should also be similar. On the other hand, it would not prove surprising if PIP_2, with its bulky, highly negatively charged headgroup, should interact with the peptide in a more specific way.

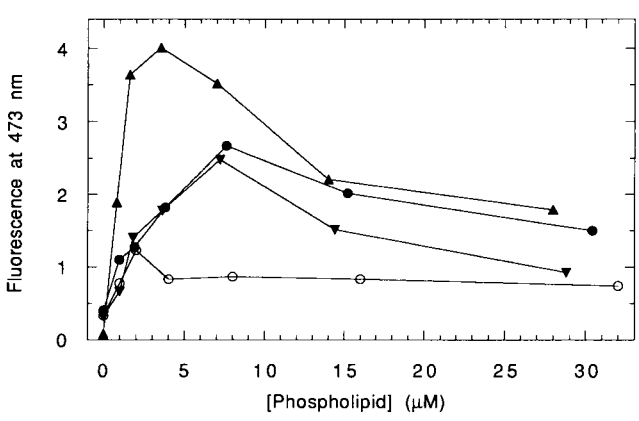

FIGURE 5 Maximal fluorescence at 473 nm, representing pyrene excimer fluorescence, of 2 mM pyrene-Cys-G(150–169) in 10 mM Tris, pH 7.0, with different concentrations of phospholipids PS (○), PIP (▼), PI (●), and PIP_2 (▲).

NMR experiments

Our NMR data show clearly that the central region of the peptide adopts a stable α-helical conformation in 50% TFE-H_2O solution. This stability manifests itself in strong NOE cross-peaks among residues 156–167 (Fig. 3). The connectivity patterns of the protons indicate short distances between α-protons and amide-protons/β-protons three residues away, a pattern unique to α-helix (Wüthrich, 1986). Medium-distance NOEs can also be observed between α-protons and amide-protons four residues away, which is also characteristic of α-helices.

Upfield shifts of α-protons are frequently observed relative to the random coil for peptides in α-helical conformations (Pastore and Saudek, 1990; Wishart et al., 1991; Zhou et al., 1993). For our peptide, such upfield shifts start from N156 and increase toward a maximum in the middle of the sequence (Fig. 2). This suggests that the helix starts at N156, stabilizes in the middle of the peptide, and becomes increasingly flexible toward the C-terminus. These chemical shift changes correspond well with the NOE crosspeak pattern (Fig. 3).

Proline residue

Cis-trans isomerization is likely to occur in dipeptide segments Xxx-Pro and Pro-Pro (Brandts et al., 1975; Ramachandran and Mitra, 1976). If the two conformers co-exist and undergo slow exchange, then two sets of resonances for proline are expected. *Cis* and *trans* Xxx-Pro conformations show different NOE patterns between proline protons and Xxx protons. In the *cis* conformation, $\alpha H_{(Xxx)}$ is close to $\alpha H_{(Pro)}$, whereas in the *trans* conformation, $\alpha H_{(Xxx)}$ is close to $\delta CH_{2(Pro)}$. In our NOESY experiments, only one set of proline resonances was observed,

indicating either that there is only one stable conformation for proline or that different conformations are undergoing rapid exchange. The fact that we observe strong NOEs between the α-proton of V154 and the δ-protons of P155 (Fig. 6) indicates that P155 is most likely to be in a stable *trans* conformation.

Prolines found in helices often occupy positions in the first turn, and more often than not they are in the N1 position (Richardson and Richardson, 1988). Dynamics simulation studies suggest that proline is stabilizing in the first helical position, which has led to the suggestion that proline can act to initiate α-helices (Yun et al., 1991). Because in G(150–169) proline appears as the first residue of the helical region, it would be interesting to examine the effect of this proline on the formation of α-helix in this peptide.

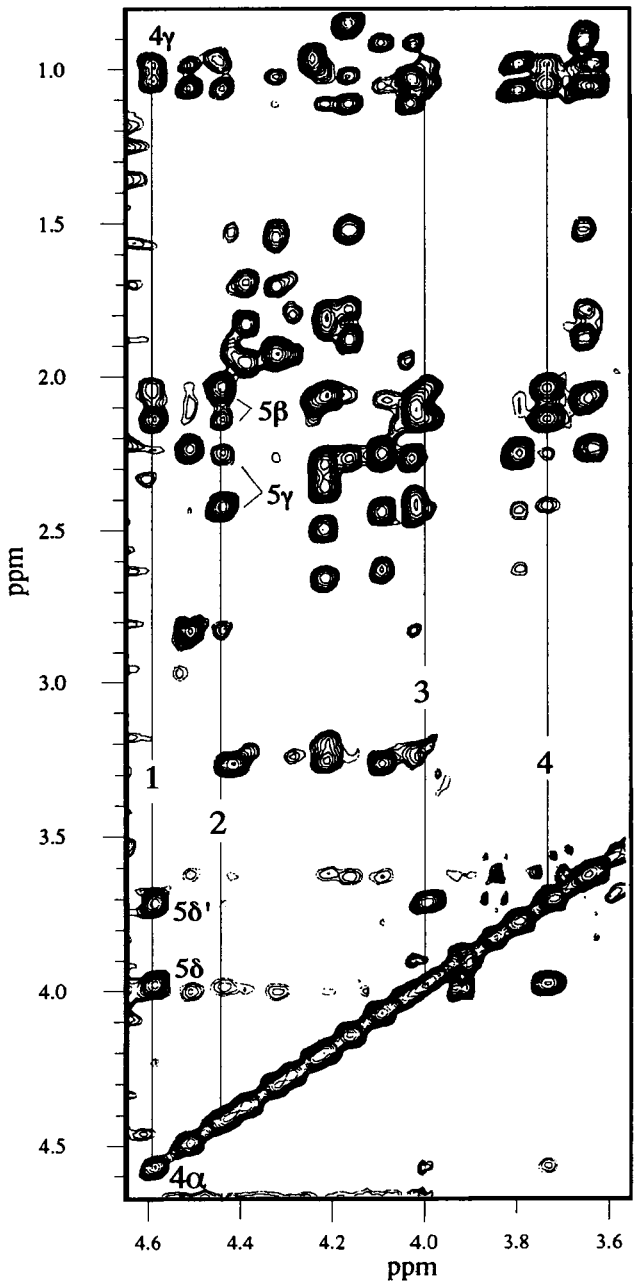

FIGURE 6 NOESY (mixing time 320 ms) spectrum of G(150–169). Lines labeled 1, 2, 3, and 4 show connectivities of 4α, 5α, 5δ, and 5δ' to other protons, respectively. On line 1, strong crosspeaks between 4α and 5δ, 5δ', 5β, and 5β' are observed, indicating a *trans* conformation of proline. On lines 2, 3, and 4 are the intra-residue NOEs of proline, suggesting that only one stable conformation of proline is likely to exist.

Molecular modeling

The RMD calculations produce a cluster of similar conformations. The central part of the peptide is well defined, reflecting the relatively abundant NOEs observed in this region. The structure of the N-terminus is poorly defined, probably because of its unstructured nature. A stereo view of the average of six selected structures is presented in Fig. 7.

The helical wheel plot of the helical region in G(150–169) is shown in Fig. 8. The wheel can be divided roughly into two sides, one side being hydrophilic and the other largely hydrophobic, rendering this helical region amphiphilic in character. This arrangement can also be visualized in the peptide model shown in Fig. 7. The side chains of five residues, V-158, V-159, L-162, F-163, and K-166, form a hydrophobic cluster on one side of the peptide backbone. One might at first glance consider K-166 an anomalous residue on the hydrophobic side of the peptide. However, a lysine residue does have a long hydrophobic alkyl chain that connects its charged amino group to the peptide backbone. Hence, K-166 should help to stabilize hydrophobic interactions, particularly if its charged side-chain tail can form a salt bridge with a charged lipid headgroup. When the peptide interacts with PIP_2, the hydrophobic side is likely to interact with the aliphatic tails of the lipids, whereas the hydrophilic side, with its multiple

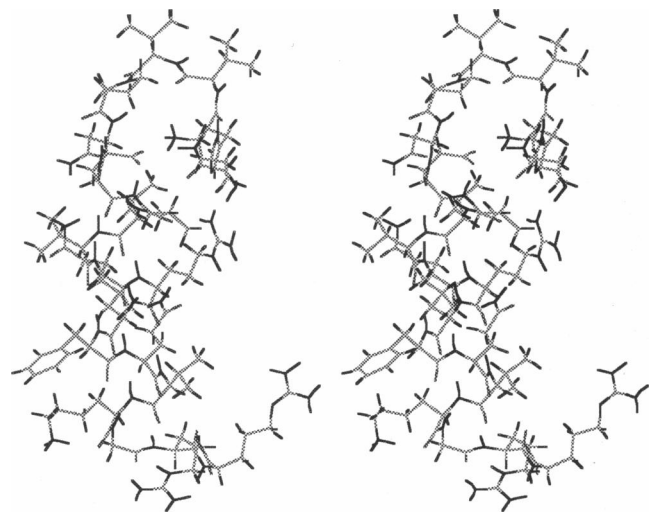

FIGURE 7 The average of structures calculated by molecular dynamics presented in stereo view.

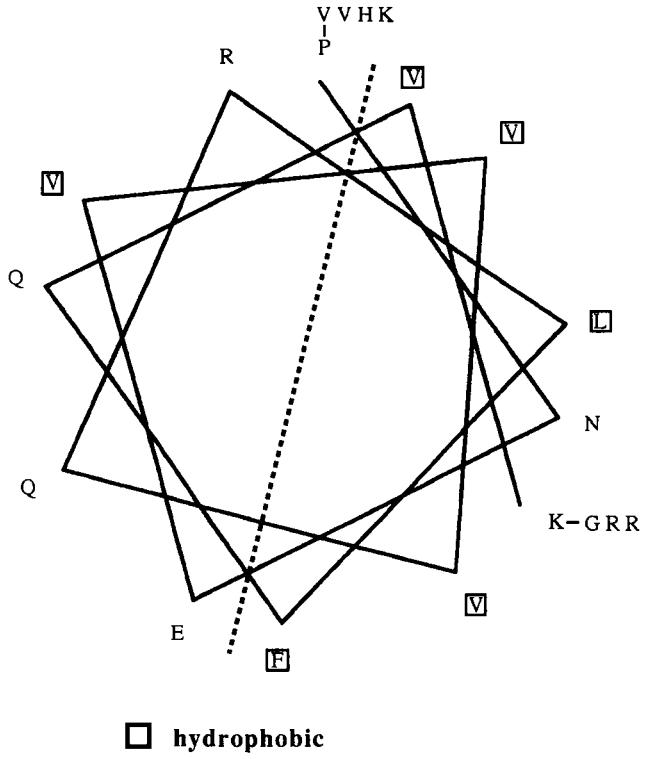

FIGURE 8 Helical wheel plot of the P-154 to K-166 region of G(150–169) with 100° angle. The dotted line shows a rough division of the molecule into polar and hydrophobic faces.

positive charges, is likely to interact with the lipid headgroups. A residue worth mentioning is Phe-163, which is positioned on the edge of the hydrophobic side of the helix and in the middle of the five-residue hydrophobic cluster. With a very bulky and hydrophobic side chain, this residue may well play an important role in the peptide-lipid interaction.

TFE-induced structure versus PIP_2-induced structure

In our study, the native structure of G(150–169) in gelsolin is unknown. It is thought to be largely unstructured in the purified protein in vitro because this peptide is one of two sites most avidly cleaved by some proteases. Indeed, a coil-helix transition induced by PIP_2 in the parent protein is one model by which phosphoinositides might inactivate gelsolin by disrupting the actin binding sites within domains 1 and 2–3, which may need to be flexibly linked to accommodate tight binding to the actin filament. Based on the conserved residues in the segment 1 core in the gelsolin family, McLaughlin et al. (1993) predicted a common fold in all six segments of gelsolin. The equivalent region to G(150–169) in segment 1 is from residues 25 to 45. The structure of this region as solved by x-ray crystallography includes a short central helix and a short segment of β-sheet toward the C-terminus.

Despite the similarities between the CD spectra of the peptide in aqueous TFE and PIP_2 micelle solutions, some structural differences are expected. For example, in PIP_2 micelle solution, interactions of the peptide with the large phospholipid headgroups will almost certainly have structural consequences. The interaction between PIP_2 and the peptide might involve any or all of electrostatic forces, hydrophobic interactions, and steric constraints. In fact, in our preliminary NMR experiments of the peptide conformation in SDS micelle solution, the proton chemical shifts of some residues are quite different from their counterparts in aqueous TFE solvent (Fig. 2), even though the CD spectrum of the peptide in SDS micelle solution is similar to that in aqueous TFE solution. The chemical shift change comparison in Fig. 2 reflects a different chemical environment for the helical conformation in SDS micelle solution, even though an interpretation of changes in chemical shifts is difficult to give because of the many factors involved. The two arginines at the C-terminus also show large upfield shift changes, which could reflect a more fixed conformation for these residues in SDS micelles compared to TFE aqueous solution. Significant differences are also evident for NOE intensities for some proton pairs in SDS micelle solution compared to those in TFE solvent. Such changes could reflect changes in the spatial arrangement and/or motional dynamics of these protons.

TFE is regarded as a helix-enhancing co-solvent rather than a helix-inducing solvent in the sense that it does not induce helix formation from random sequences, but rather for sequences with intrinsic helical propensities (Lehrmann et al., 1990; Sönnichsen et al., 1992). According to the secondary structure predictions using the Chou-Fasman method, the middle segment of G(150–169) has a propensity to form β-sheet; but the consensus result of the SOPM method shows that the middle region of the peptide possesses helix-forming potential (Table 2). This predicted helical region corresponds to the experimental results quite well. Anionic lipids are also known to induce helix formation of peptides (Pasta et al., 1990; Wu and Yang, 1981). It has been hypothesized that the conformation of peptides in surfactant solutions depends on their structure-forming potential (Wu and Yang, 1981). Therefore, the similarity between the two conformations reflects the structure-forming potential of the peptide, whereas the difference between the two conformations will reveal the hydrophobic, electrostatic, and steric effect of the lipid environment on the peptide structural transition.

TABLE 2 Secondary structure predictions for G(150–169)

Sequence	K	H	V	V	P	N	E	V	V	V	Q	R	L	F	Q	V	K	G	R	R
*Chou-Fasman	C	C	C	C	T	T	C	B	B	B	B	B	B	B	B	B	C	C	C	C
‡SOPM consensus	C	B	B	C	C	C	H	H	H	H	H	H	H	H	H	H	C	C	C	C

*Chou and Fasman, 1978; Nishikawa, 1983.
‡Geourjon and Deleage, 1994.
B, β-sheet; C, random coil; H, helix; T, turn.

Fluorescence experiments

Although a systematic structural comparison of this and similar peptides in lipid environments of variable composition awaits further studies, our fluorescence data nonetheless provide some crucial insight into the nature of the interactions. We believe these data to be relevant because the relative disorder of the G(150–169) peptide N-terminus suggests that the pyrene label may not strongly perturb the conformational changes of the peptide involving α-helix formation in the middle of the sequence.

The main implication of the effects of different phospholipids on pyrene-labeled fluorescence is the evidence for cluster formation caused specifically by phosphoinositides. All negatively charged amphiphiles we have examined, including SDS (data not shown), have some effects on the fluorescence emission of the monomeric pyrene-peptide adducts, but only phosphoinositides, and especially PIP_2, have a strong tendency to aggregate the peptides at a narrow range of peptide/lipid ratios. The peptides remain soluble, and no turbidity is observed at the low concentrations used. The excimer fluorescence disappears when larger amounts of PIP_2 are added, suggesting that the cluster formation is a dynamic process and occurs only when the surface of phosphoinositide-containing structures is crowded with bound peptides. The ability to form clusters of PIP_2 headgroups bound to protein ligands in the cell membrane may be a biologically relevant aspect of the function of these acidic lipids (Janmey, 1995, to be submitted).

Dr. R. Shoemaker is gratefully acknowledged for help with the NMR experiments, with the molecular modeling software, and for useful discussions. Dr. T. Garver is thanked for help in the initial stages of the project, and Dr. J. J. Stezowski is thanked for use of his molecular modeling hardware and software.

This work is supported by a grant from the Biotechnology Center of the University of Nebraska-Lincoln to William H. Braunlin, and grants from the National Institutes of Health (AR38910) and the Fogarty Foundation to Paul A. Janmey.

REFERENCES

Bax, A., and D. G. Davis. 1985. MLEV-17-based two-dimensional homonuclear magnetization transfer spectroscopy. *J. Magn. Reson.* 65: 355–360.

Bax, A., R. Freeman, and G. Morris. 1981. Correlation of proton chemical shifts by two-dimensional Fourier transform NMR. *J. Magn. Reson.* 42:164–168.

Brandts, J. F., H. R. Halvorson, and M. Brennan. 1975. Consideration of the possibility that the slow step in protein denaturation reactions is due to cis-trans isomerism. *Biochemistry.* 14:4953–4963.

Braunschweiler, L., and R. R. Ernst. 1983. Coherence transfer by isotropic mixing: application to proton correlation spectroscopy. *J. Magn. Reson.* 53:521–528.

Brown, S. C., P. L. Weber, and L. Mueller. 1988. Toward complete ^1H NMR spectra in proteins. *J. Magn. Reson.* 77:166–169.

Chou, P. Y., and G. D. Fasman. 1978. Empirical predictions of protein conformation. *Annu. Rev. Biochem.* 47:251–276.

Clark, M., R. D. Cramer III, and N. Van Opdenbosch. 1989. Validation of the general purpose Tripos 5.2 force field. *J. Comp. Chem.* 10:982–1012.

Crippen, G. M., and T. F. Havel. 1988. Distance Geometry and Molecular Conformation. Wiley, New York.

Geourjon, C., and G. Deleage. 1994. SOPM: a self optimized prediction method for protein secondary structure prediction. *Protein Eng.* 7:157–164.

Haugland, R. P. 1992. Molecular probes. *In* Handbook of Fluorescent Probes and Research Chemicals. Molecular Probes, Inc., Eugene, OR. 16.

Janmey, P. A. 1993. A slice of the actin. *Nature.* 364:675–676.

Janmey, P. A., J. Lamb, P. G. Allen, and P. T. Matsudaira. 1992. Phosphoinositide-binding peptides derived from the sequences of gelsolin and villin. *J. Biol. Chem.* 267:11818–11823

Janmey, P. A., and T. P. Stossel. 1987. Modulation of gelsolin function by phophatidylinositol 4,5-bisphosphate. *Nature.* 325:362–364.

Lehrman, S. R., J. L. Tuls, and M. Lund. 1990. Peptide α-helicity in aqueous trifluoroethanol: correlations with predicted α-helicity and the secondary structure of the corresponding regions of bovine growth hormone. *Biochemistry.* 29:5590–5596.

Llinas, M., and M. P. Klein. 1975. A proton magnetic resonance study of solvation effects on the amide electron density distribution. *J. Am. Chem. Soc.* 97:4731–4737.

Macura, S., Y. Huang, D. Suter, and R. Ernst. 1982. Two-dimensional chemical exchange and cross-relaxation spectroscopy of coupled nuclear spins. *J. Magn. Reson.* 43:259–281.

McLaughlin, P. J., J. T. Gooch, H.-G. Mannherz, and A. G. Weeds. 1993. Structure of gelsolin segment 1-actin complex and the mechanism of filament severing. *Nature.* 364:685–692.

Morris, G. A., and R. Freeman. 1978. Selective excitation in Fourier transform nuclear magnetic resonance. *J. Magn. Reson.* 29:433–462.

Nelson, J. W., and N. R. Kallenbach. 1986. Stabilization of the rebonuclease S-peptide α-helix by trifluoroethanol. *Proteins.* 1:211–217.

Nishikawa, K. 1983. Assessment of secondary-structure prediction of proteins: comparison of computerized Chou-Fasman method with others. *Biochim. Biophys. Acta.* 748:285–299.

Pasta, P., G. Carrea, R. Longhi, and L. Zetta. 1990. Circular dichroism and proteolysis of human b-endorphin in surfactant and lipid solutions. *Biochim. Biophys. Acta.* 1039:1–4.

Pastore, A., and V. Saudek. 1990. The relationship between chemical shift and secondary structure in proteins. *J. Magn. Reson.* 90:165–176.

Ramachandran, G. N., and A. K. Mitra. 1976. An explanation for the rare occurrence of cis peptide units in proteins and polypeptides. *J. Mol. Biol.* 107:85–92.

Richardson, J. S., and D. C. Richardson. 1988. Amino acid preference for specific locations at the ends of α helices. *Science.* 240:1648–1652.

Sönnichsen, F. D., J. E. Van Eyk, R. S. Hodges, and B. D. Sykes. 1992. Effect of trifluoroethanol on protein secondary structure: an NMR and CD study using a synthetic actin peptide. *Biochemistry.* 31:8790–8798.

Wishart, D. S., B. D. Sykes, and F. M. Richards. 1991. Relationship between nuclear magnetic resonance chemical shift and protein secondary structure. *J. Mol. Biol.* 222:311–333.

Wu, C-S. C., and J. T. Yang. 1981. Sequence-dependent conformations of short polypeptides in a hydrophobic environment. *Mol. Cell. Chem.* 40:109–122.

Wüthrich, K. 1986. NMR of Proteins and Nucleic Acids. Wiley, New York.

Yang, J. T., C. C. Wu, and H. M. Martinez. 1986. Calculation of protein conformation from circular dichroism. *Methods Enzymol.* 130:206–269.

Yu, F. X., H. Q. Sun, P. A. Janmey, and H. L. Yin. 1992. Identification of a polyphosphoinositide-binding sequence in an actin monomer-binding domain of gelsolin. *J. Biol. Chem.* 267:14616–14621.

Yun, R. H., A. Anderson, and J. Hermans. 1991. Proline in α-helix: stability and conformation studied by dynamics simulation. *Proteins.* 10:219–228.

Zhou, N. E., C. M. Kay, B. D. Sykes, and R. S. Hodges. 1993. A single-stranded amphipathic α-helix in aqueous solution: design, structural characterization, and its application for determining α-helical propensities of amino acids. *Biochemistry.* 32:6190–6197.